ASYMMETRIC IMPACT OF A TWO-DIMENSIONAL LIQUID COLUMN

B.S. Yoon, Y.A. Semenov

School of Naval Architecture and Ocean Engineering University of Ulsan, Republic of Korea
E-mail: bsyoon@ulsan.ac.kr, semenov@a-teleport.com

ABSTRACT

The hydrodynamic impact of a two-dimensional liquid column is analyzed on the basis of a generalized solution of a water impact between a liquid and a solid wedge. The liquid is assumed to be ideal and incompressible; gravity and surface tension effects are ignored. The flow generated by the impact is two-dimensional and potential. The solution is based on two governing expressions, namely, the complex velocity and the derivative of the complex potential. These expressions are derived in an auxiliary parameter plane using integral formulae for solving mixed and homogeneous boundary-value problems in the first quadrant of the auxiliary plane. The system of an integral and an integro-differential equation in the velocity modulus and the velocity angle with respect to the free surface is derived by using the dynamic and kinematic boundary conditions. A numerical procedure for solving these equations is carefully validated by using the fact that the oblique impact of a liquid wedge onto a flat solid surface is invariant under the choice of a system of coordinates. The results are presented in terms of the free surface shape, streamlines and pressure distribution on the solid surface.

I. INTRODUCTION

During the last decade, practical needs involving the design of ships, offshore platforms and high-speed vessels have regenerated interest in research on unsteady hydrodynamic effects which may lead to heavy hydrodynamic loads on vessels and their structural elements. Green water on a ship deck, slamming, and wave impact on offshore platforms and the coastline are examples. In many practical cases, at the initial stage of a fluid–structure impact characterized by the largest loading the flow can be considered as self-similar.

A solid wedge entering a flat free surface is often used in mathematical and numerical simulation of impact [1 – 5]. A closely related problem is the impact of a liquid wedge on a solid wall, which was considered by Cumberbatch using the self-similar method [6]. A similar problem was solved analytically by Howison *et al.* [7] using the method of matched asymptotic expansions. Basic characteristics of jet impact were studied by Korobkin [8]. Semenov [9] and Wu [10] solved the problem for the case of a symmetric flow configuration using analytical methods of the calculus of complex variables [9] and the complex velocity potential together with the boundary-element method [10]. Faltinsen *et al.* [11] developed a fully nonlinear numerical method and studied in details the impact of green water on a deck and a vertical deck-house wall in the bow area.

In the present study we consider a two-dimensional liquid column with an arbitrary orientation with respect to a solid boundary and an oblique velocity component. The solid boundary may be flat or cornered. An advanced hodograph method is applied to derive analytical expressions for two governing functions, which are the complex velocity and the derivative of the complex potential, both defined in the first quadrant of the parameter plane. From these expressions the complex potential for wedge entry into a flat free surface is obtained as a special case.

These governing functions include the velocity magnitude and the velocity angle with respect to the free surface, which are determined from dynamic and kinematic boundary conditions. These conditions in terms of the velocity magnitude and angle with respect to the free surface are common to self-similar problems, and they have been derived in [3].

An arbitrary orientation of the liquid wedge relative to the solid wedge and an oblique velocity component provide special conditions to check the validity of computations. By considering a solid wedge of angle π (that corresponds to a flat solid surface) and a liquid wedge oriented symmetrically with respect to the solid surface having a horizontal velocity component, we should obtain the same pressure distribution along the solid surface irrespective of the oblique angle determined by the horizontal velocity component of the solid surface. On the other hand, the streamlines and the velocity magnitude and angle with respect to the free surface depend on the oblique angle. This will be shown in the following.

2. GOVERNING EXPRESSIONS

The fluid is assumed to be incompressible and inviscid, and the flow is assumed to be irrotational. A sketch of the flow and the definitions of the geometric parameters are shown in Fig. 1.

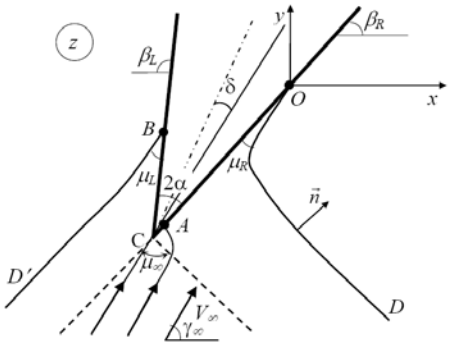

Figure 1. Sketch of an impact between a liquid (dashed line) and a solid wedge

The governing expressions, which are the complex velocity and the derivative of the complex potential, for the self-similar problem of the-entry of a wedge into a liquid with a flat free surface have been derived in [4]. For the present study of the wedge-shaped region of the inflow, the expression for the complex velocity is the same because the points where the velocity is equal to zero or infinity are the same. The derivative of the complex potential differs in the order of singularity at infinity, to which the points $\varsigma = \pm i$ in the parameter plane correspond. By using the method developed in [4], it is possible to determine the order of singularity at infinity for the wedge-shaped inflow region, which is $1+\mu_\infty/\pi$. If the angle of the liquid wedge $\mu_\infty = \pi$, then the order of singularity becomes equal to 2, and expression (2) for the derivative of the complex potential coincides with that derived in [4] for a flat free surface. Thus, the governing expressions have the following form for the complex velocity

$$\frac{dw}{dz} = e^{-i(\gamma_\infty+\alpha+\delta)}\left(\frac{\varsigma-a}{\varsigma+a}\right)\left(\frac{\varsigma+c}{\varsigma-c}\right)^{(1-2\alpha/\pi)} \exp\left[-\frac{i}{\pi}\int_0^\infty \frac{d\ln v}{d\eta}\ln\left(\frac{i\eta-\varsigma}{i\eta+\varsigma}\right)d\eta\right]. \quad (1)$$

and for the derivative of the complex potential

$$\frac{dw}{d\varsigma} = N\frac{\varsigma^{(2\mu_R/\pi-1)}(\varsigma^2-a^2)}{\left(1+\varsigma^2\right)^{(1+\mu_\infty/\pi)}}\exp\left[-\frac{1}{\pi}\int_0^\infty \frac{d\theta}{d\eta}\ln\left(\eta^2+\varsigma^2\right)d\eta\right]. \quad (2)$$

Here, the parameters N, a, c are determined from physical conditions, and the functions $v(\eta)$ and $\theta(\eta)$ are determined from the dynamic and kinematic boundary conditions (see reference [4]).

If these functions are known, the velocity field and the relation between the parameter region and the physical flow region can be determined as follows:

$$z(\varsigma) = z(0) + \int_0^\varsigma \frac{dw}{d\varsigma}\Big/\frac{dw}{dz}d\varsigma, \qquad v_x - iv_y = \frac{dw}{dz}(\varsigma) \quad (3)$$

where v_x and v_y are the x - and y - components of the velocity. Once the function $\theta(\eta)$ is evaluated, the contact angles between the wedge sides and the free surface, μ_R and μ_L, can be determined as follows: $\mu_R = \lim_{\eta\to 0}\theta(\eta)$, $\mu_L = \pi - \lim_{\eta\to\infty}\theta(\eta)$.

3. ANALYSIS OF THE FLOW PARAMETERS

Figure 2*a* shows the streamline patterns for an impact between a concave solid corner with half-angle $\alpha = 7\pi/9$ and a liquid wedge of angle $\mu_\infty = 2\pi/9$. As illustrated,

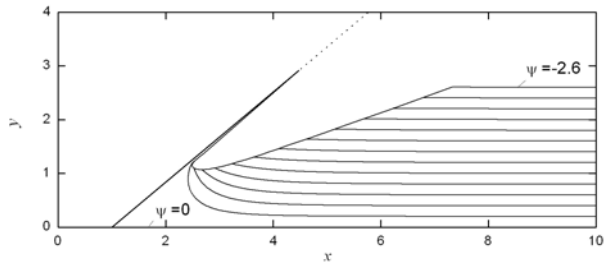

(*a*)

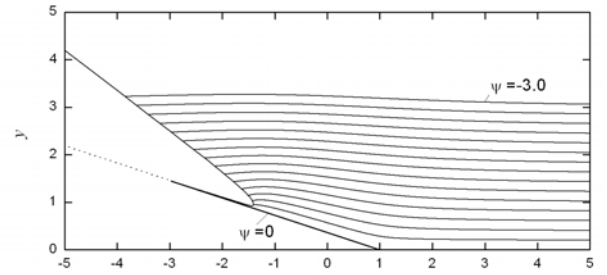

(*b*)

Figure 2: Streamline patterns corresponding to $\alpha = 7\pi/9$, $\mu_\infty = 2\pi/9$ (a) and $\alpha = \pi/9$, $\mu_\infty = 14\pi/9$

the first streamline $\psi = -0.2$ swings to the tip jet at quite a large distance from the corner. This means that the velocity magnitude in the space between the streamlines $\psi = 0$ and $\psi = -0.2$ near the corner is quite small. Another example is shown in Figure 2b for a solid wedge of half-angle $\alpha = \pi/9$ (acute angle) and a liquid concave wedge of angle $\mu_\infty = 14\pi/9$. When the lengths of the tip jets in figures 2a and b are compared, it is apparent that the tip jet is longer for case (a), which corresponds to the higher value of the velocity.

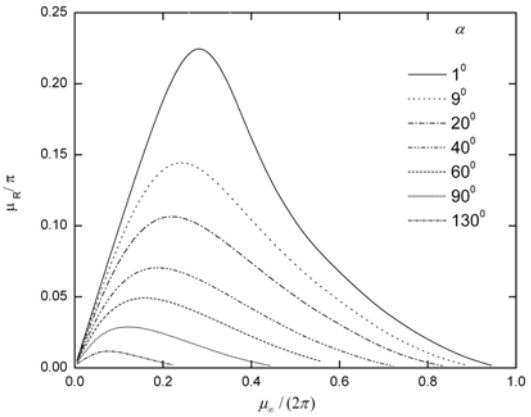

Figure 3: Contact angle for a solid wedge of angle α as a function of the angle of the liquid wedge μ_∞.

Figure 3 shows the contact angle for a symmetric impact as a function of the angle of the liquid wedge. The smaller the angle of the solid wedge, the larger the angle of the tip jet at the contact point. The largest value of the contact angle tends to 45 degrees for the case of a thin solid wedge and a liquid wedge of angle 45 degrees too. The maximal value of 45 degrees for the contact angle was estimated by Dobrovolskaya [1].

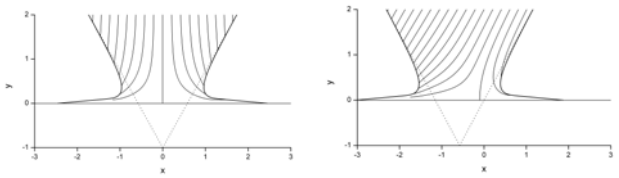

(a) (*b*)

Figure 4: Streamline patterns for a symmetrically orientated liquid wedge of angle $\mu_\infty=60^0$ impacting a solid flat surface at oblique angles $\gamma = 90^0$ (*a*) and $\gamma=60^0$ (*b*).

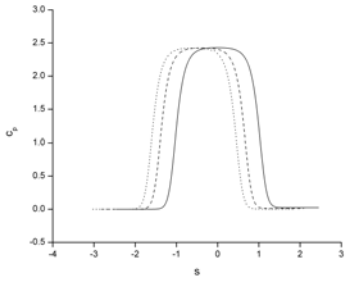

Figure 5. Pressure coefficient along the solid surface for cases (*a*) (solid line) and (*b*) (dotted line) in Figure 4.

In Figure 4, a liquid wedge of angle $\mu_\infty=60^0$ has a symmetric orientation with respect to a flat solid surface (the angle of the solid wedge $\alpha=90^0$). The horizontal component of the impact velocity forms oblique angle $\gamma=90^0$ for case (a) and $\gamma=60^0$ for case (b). It can be seen that the free surfaces on the left and on the right remain symmetric during the impact. Indeed, in a system of coordinates fixed to the liquid wedge, the flat solid surface will have a horizontal velocity component, which does not affect the impact. This is also confirmed by Figure 5, which shows the pressure distribution on the solid surface. As illustrated, the pressure distribution is only shifted relative to the point x=0 where the liquid wedge touches the solid surface at the initial time.

Figure 6 shows the streamline patterns for different orientations of a liquid wedge impacting a solid surface in the vertical direction. The corresponding pressure distributions are shown in Figure 7. The behavior of the pressure distribution is similar to wedge entry into a liquid with a flat free surface. The pressure and the velocity in the tip jet increase near the jet root on the side with the smaller deadrise angle.

Figure 8 shows the streamline pattern for the case of oblique impact of a liquid wedge with the velocity directed along its symmetry axis. As illustrated, the position of the stagnation point is closer to the root of the tip jet on the side with the smaller deadrise angle.

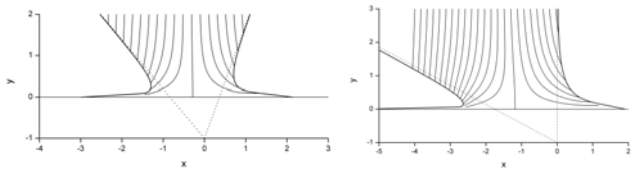

Figure 6: Vertical impact of a liquid wedge of angle $\mu_\infty=60^0$ rotated through angles $\delta = 10^0$ (*a*), $\delta = 30^0$ (*b*).

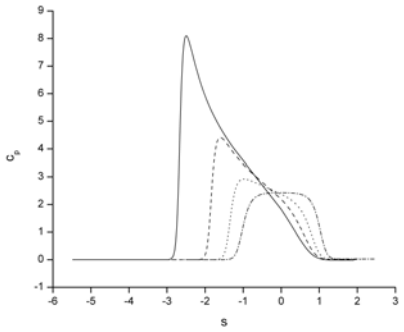

Figure 7: Pressure distribution along the solid surface for vertical impact: $\delta = 0$ (dash dotted line), $\delta = 10^0$ (dotted line), $\delta = 20^0$ (dashed line) and $\delta = 30^0$ (solid line).

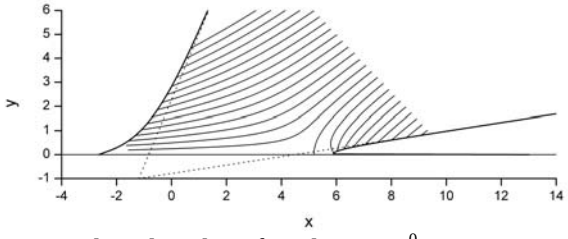

Figure 8. A liquid wedge of angle $\mu_\infty=60^0$ impacting a solid surface at angle $\gamma = 40^0$.

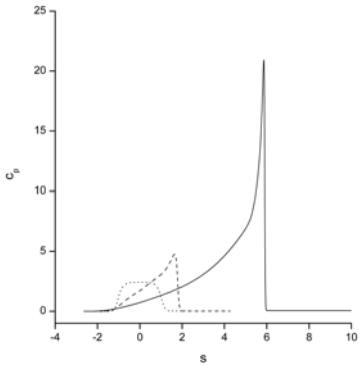

Figure 9. Pressure distribution along the solid surface for the case of oblique impact: impact angle $\gamma = 90^0$ (dotted line), $\gamma=60^0$ (dashed line) and $\gamma=40^0$ (solid line).

Figure 9 shows the pressure distributions along the solid surface for the case of oblique impact. The pressure peak appears on the side with the smaller deadrise angle. The pressure distribution is qualitatively similar to the case of vertical impact of an asymmetric liquid wedge shown in Figure 7.

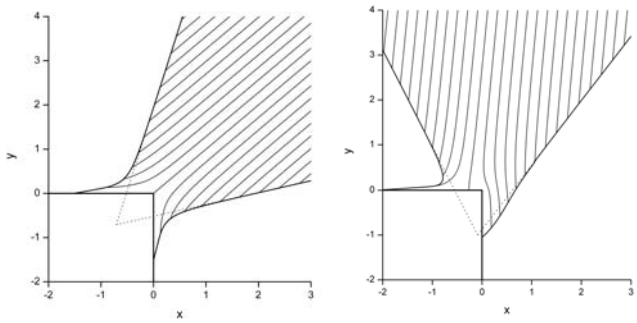

(*a*) (*b*)

Figure 10: Impact between a solid wedge of half-angle $\alpha=45^0$ and a liquid wedge of angle $\mu_\infty=60^0$ symmetric about the velocity direction and rotated through angles $\delta = 0$ (*a*) and $\delta = 40^0$ (*b*).

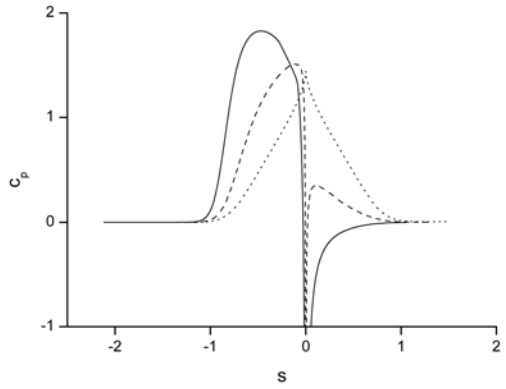

Figure 11: Pressure distribution along the sides of the solid wedge for $\delta = 0, 20^0, 40^0$ shown by dotted/dashed/solid lines, respectively.

Figure 10 shows the streamline patterns for an impact between a liquid wedge and a solid wedge of angle $2\alpha=90^0$. The tip of the corner and the vertex of the liquid wedge touch each other at initial time t=0. Figure 10b shows the flow configuration corresponding to the largest angle of rotation of the liquid wedge, for which the iterative solution of the integral equations converges and the contact angle on the right side tends to 45 degrees. For larger angles of rotation flow separation may occur at the solid corner. This is confirmed by the pressure distribution shown in Figure 11 as a solid line. As illustrated, the pressure along the right side of the solid square becomes negative along the whole length of the wetted side and increases monotonically to the pressure on the free surface. Such a pressure distribution provides conditions for ventilation and, consequently, for flow separation from the vertex of the solid square.

3. CONCLUSIONS

The initial stage of an oblique impact between a liquid and a solid wedge has been investigated in a wide range of inflow conditions. The study is based on the derivation of an analytical expression for the complex potential of the flow and the numerical solution of the system of integral and integro-differential equations in the unknown velocity magnitude and angle with respect to the free surface.

The presented results show that the pressure distribution along the solid surface is similar to that occurring during wedge entry into a flat free surface. The main parameter determining the pressure peak is the angle between the solid and the free surface, or the deadrise angle. The smaller the deadrise angle, the higher the pressure peak. At a fixed deadrise angle, the pressure peak increases with the angle of the solid wedge, which corresponds to the cumulative effect.

4. REFERENCES

1. Dobrovol'skaya, Z.N., 1969. On some problems of similarity flow of fluid with a free surface. Journal Fluid Mechanics 36, 805–829.
2. Zhao, R. & Faltinsen, O. 1993 Water-entry of two dimensional bodies. J. Fluid Mech. **246**, 593–612.
3. Zhang, S., Yue, D. K. P., and Tanizawa, K., (1996) Simulation of Plunging Wave Impact on a Vertical Wall. J. Fluid Mech., **327**, pp. 221–254.
4. Semenov, Y.A., Yoon B.S. (2009) Onset of Flow Separation at Oblique Water Impact of a Wedge. Physics of Fluids, **21**, pp. 112103 – 11.
5. Xu, G.D., Duan, W.Y. and Wu, G.X. (2008) Similarity solution for wedge-shaped fluid/structure impact. IWWWFB, Seoul. www.iwwwfb.org
6. Cumberbatch, E. (1960) The impact of a water wedge on a wall, *J. Fluid Mech.* **7** 353–374.
7. Howison, S. D., Ockendon, J. R., Oliver, J. M., Purvis, R. and Smith, F. T. (2005) Droplet impact on a thin fluid layer, *J. Fluid Mech.* **542**, pp. 1–23.
8. Korobkin, A.A., (1996) Global characteristics of jet impact. Journal of Fluid Mechanics, 307, 63–84.
9. Semenov, Y.A. (2004) Method for solving nonlinear problems on unsteady free-boundary flows. XXI International Congress of Theoretical and Applied Mechanics, 15 – 21 August, Warsaw.
10. Wu, G.X. (2007) Two-dimensional liquid column and liquid droplet impact on a solid wedge. Q. J. Mech. Appl. Math, **60**, No. 4, pp. 497 – 511.
11. Faltinsen, O. M., Greco, M. and Landrini, M. (2002) Green Water Loading on a FPSO. ASME J. of Offshore Mechanics and Arctic Engineering, 122, pp. 97 – 103.